Article

Activation of the NLRP3 Inflammasome by Hyaboron, a new Asymmetric Boron-Containing Macrodiolide from the Myxobacterium *Hyalangium minutum*

Frank Surup, Dhruv Chauhan, Jutta Niggemann, Eva Bartok, Jennifer Herrmann, Matthias Keck, Wiebke Zander, Marc Stadler, Veit Hornung, and Rolf Müller

ACS Chem. Biol., **Just Accepted Manuscript** • DOI: 10.1021/acschembio.8b00659 • Publication Date (Web): 05 Sep 2018

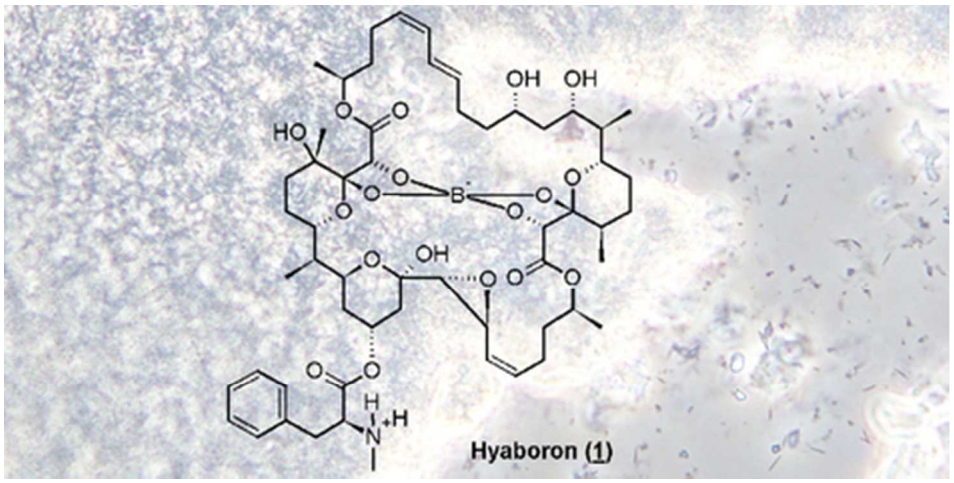

39x19mm (300 x 300 DPI)

Activation of the NLRP3 Inflammasome by Hyaboron, a new Asymmetric Boron-Containing Macrodiolide from the Myxobacterium *Hyalangium minutum*

Frank Surup,[‡,⊥,+] Dhruv Chauhan,[†,+] Jutta Niggemann,[‡] Eva Bartok,[§] Jennifer Herrmann,[∥,⊥] Matthias Keck,[‡,▽] Wiebke Zander,[‡,○] Marc Stadler,[‡,⊥] Veit Hornung,*[,†,#] and Rolf Müller*[,‡,∥,⊥]

[‡]Helmholtz Center for Infection Research (HZI) Department Microbial Drugs Inhoffenstraße 7, 38124 Braunschweig, Germany

[†]Gene Center and Department of Biochemistry, Ludwig-Maximilians-Universität München, Munich, Feodor-Lynen-Straße 25, Munich, 81377, Germany

[§]Institute of Clinical Chemistry and Clinical Pharmacology, University Hospital, Sigmund-Freud-Straße 25, University of Bonn, 53127 Bonn, Germany

[∥]Helmholtz Institute for Pharmaceutical Research Saarland (HIPS), Helmholtz Center for Infection Research and Department of Pharmacy, Saarland University Campus, Building E8.1, 66123 Saarbrücken, Germany

[⊥]German Centre for Infection Research Association (DZIF), partner site Hannover-Braunschweig, Inhoffenstraße 7, 38124 Braunschweig, Germany

[#]Center for Integrated Protein Science (CIPSM), Ludwig-Maximilians-Universität München, Munich, Feodor-Lynen-Straße 25, Munich, 81377, Germany

ABSTRACT: A Natural Compound Library containing myxobacterial secondary metabolites was screened in murine macrophages for novel activators of IL-1β maturation and secretion. The most potent of three hits in total was a so far undescribed metabolite, which was identified from the myxobacterium *Hyalangium minutum* strain Hym3. While the planar structure of **1** was elucidated by HRMS and NMR data yielding an asymmetric boron containing macrodiolide core structure, its relative stereochemistry of all 20 stereo centers of the 42-membered ring was assigned by ROESY correlations, $^{1}H,^{1}H$ and $^{1}H,^{13}C$ coupling constants, and by comparison of ^{13}C chemical shifts to those of the structurally related metabolites tartrolon B-D. The absolute stereochemistry was subsequently assigned by Mosher's and Marfey's methods. Further functional studies revealed that hyaboron and other boronated natural compounds resulted in NLRP3 inflammasome dependent IL-1β maturation, which is most likely due to their ability to act as potassium ionophores. Moreover, besides its inflammasome-stimulatory activity in human and mouse cells, hyaboron (**1**) showed additional diverse biological activities, including antibacterial and antiparasitic effects.

The human immune system continuously encounters various pathogens. These threats are detected at the molecular level via the so-called pathogen recognition receptors (PRR) of the innate immune system, which sense the distinct pathogen associated molecular patterns (PAMP) of invading microorganisms. The distinction between self and non-self molecules is critical to pathogen recognition and clearance. Nonetheless, the immune system is not always capable of eradicating pathogenic microorganisms on its own.[1] Antibiotics are a vital therapeutic approach to the treatment of many bacterial infections. These compounds specifically act against bacterial processes and targets such as cell wall synthesis or transcriptional and translational machineries.[2] However, the extensive use of broad-spectrum antibiotics in past years has resulted in the emergence of multi-drug resistant pathogens.[3] Therefore, the struggle against bacterial pathogens urgently calls for novel strategies such as narrow-spectrum antibiotics, which are effective against selective species of one bacterial class, as well as the use of adjuvant immunotherapies for the activation of the host immune system.[4] Since broad immune activation could be detrimental to the host, targeted immunotherapies are needed, yet such approaches require detailed knowledge of which pathways control protective immune responses and which are responsible for inappropriate tissue damage at the site of infection.[5]

The inflammasome-dependent interleukin-1β (IL-1β) pathway plays an important role in the control and elimination of bacterial pathogens.[6] Inflammasomes are cytosolic, macromolecular complexes which are formed upon sensing PAMPs or danger associated molecular patterns (DAMPs).[7] Inflammasome complexes typically consist of a sensor protein such as a NOD-like receptor (e.g. NLRP3), the adapter molecule ASC (apoptosis associated speck like protein containing caspase activation and recruitment domain) and the protease caspase-1. Upon activation, the sensor protein acts as a seed to initiate the prion-like formation of large filamentous ASC structures. In turn, these ASC filamentous structures recruit and activate caspase-1, which then catalyzes the proteolytic

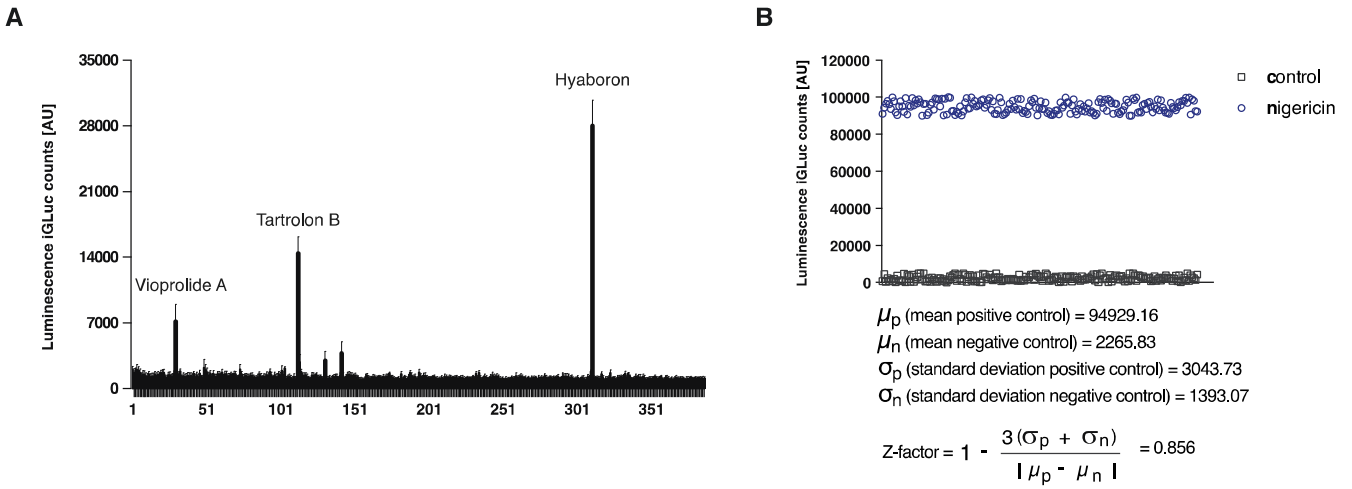

Figure 1. (A) *Natural Compound Library* of the DZIF was screened (1 μM) using J774 macrophage cell line stably transduced with iGLuc and constitutively expressing NLRP3. The iGLuc signal was measured in supernatant after 2 hr. The figure is representative of two independent experiments performed in duplicate. Error bars represent mean + SEM. AU, arbitrary units. (B) Calculations of Z-factor of iGLuc screening.

maturation of interleukin-1β (IL-1β) and its family member IL-18.[7] In general, activation of inflammasomes is a two-step process where signal 1 acts as the priming signal to induce the expression of pro-IL-1β and signal 2 is required to activate inflammasome sensor itself. Additionally, for the NLRP3 inflammasome, signal 1 facilitates priming of NLRP3 expression as well as its activation at transcriptional and post-transcriptional level.[8,9]

To identify novel immune adjuvants for anti-infective therapies or targeted modulators of the host immune system we screened the *Natural Compound Library* (NCL) of the German Centre for Infection Research (DZIF), a collection of 259 purified small molecules (compound number at the time point of screening, 2013/2014) derived from myxobacteria and other natural sources for their ability to induce IL-1β secretion (Figure 1A). The library was provided in a ready-to-screen format by the Thematic Infrastructure (TI) NCL, which is now part of the Thematic Translational Unit (TTU) Novel Antibiotics of DZIF.

To this end, we utilized J774 immortalized murine macrophages that were stably transduced with iGLuc, a Gaussia luciferase-based proteolytic reporter for inflammasome activity.[10] The iGLuc reporter allowed the measurement of Gaussia luciferase activity as a readout for proteolytic IL-1β maturation.[10,11] Additionally, we stably transduced the cell line with NLRP3 under the constitutive EF1α promoter, which eliminated the need for NF-kB priming of NLRP3 expression prior to compound screening.[8,12] In our screening system, stimulation with the NLRP3 activator nigericin yielded a Z-factor of 0.84 (Figure 1B).[13-15] The hit threshold for activation was then defined as luciferase activity more than three standard deviations from the mean of all wells. Two independent screenings resulted in the reproducible identification of three activators: vioprolide A,[16] tartrolon B[17] and hyaboron (**1**, Figure 1A), corresponding to 1.1% of compounds screened. Interestingly, hyaboron (**1**), the strongest hit, was previously isolated but not structurally elucidated in our laboratory. Consequently, we decided to perform a comprehensive structural examination, and **1** was isolated from the extracts of *Hyalangium minutum*, strain Hym3. The quasimolecular HRESIMS ion peak at *m/z* 1068.5710 provided the molecular formula $C_{56}H_{82}BNO_{18}$. The presence of boron was deduced from a characteristic [M-1] peak with 25% intensity in the molecular ion cluster.

After isolation of 15.6 mg of hyaboron (**1**) from a large scale fermentation, proton and $^{1}H,^{13}C$ HSQC spectra revealed the existence of seven methyl, 14 methylene, nine olefinic/aromatic methine (two with dual intensity), and 15 aliphatic methine groups, leaving six exchangeable protons. The carbon spectrum resolved 11 additional carbon atoms: three carbonyls, one sp^2 and four oxygenated sp^3 hybridized quaternary carbons. $^{1}H,^{1}H$ COSY and TOCSY correlations showed five spin systems (Figure S1, Table S1). The largest ones were connected by $^{1}H,^{13}C$ HMBC correlations (Figure S1) to form the 42-membered core structure characteristic for tartrolon-type metabolites. An additional six-membered ring structure was deduced by the HMBC correlation between 9–H and C–13. A protonated *N*-methylphenylalanyl side chain, forming an inner ion pair with the boron-core structure, was assigned and connected to C–11 due to a HMBC correlation from 11–H to C–1". The C–14/C–15 epoxide was indicated by the high field shifts of oxymethines 14–H (δ_H 2.81) and 15–H (δ_H 3.10), and further authenticated by large $^{1}J_{H14C14}$ and $^{1}J_{H15C15}$ values of 177 and 174 Hz, respectively. Vicinal coupling constants of 11.4 Hz indicated *Z* configurations of the $\Delta^{16,17}$ and $\Delta^{16',17'}$ double bonds, while the coupling constant of 14.2 Hz suggested the *E* configuration of the $\Delta^{14',15'}$ double bond.

The relative configuration of **1** was derived from ROESY correlations, analysis of coupling constants and comparison of carbon chemical shifts to those of tartrolon B and C, for which detailed NMR analyses and crystal structures are available.[16,17] Particularly, the six-membered ketal rings had the alkyl substituents at C–3, C–4, C–7 and C–3', C–4', C–7', respectively, in all equatorial positions according to diaxial ROESY correlations (Figure S2). ROESY correlations between 4–OH and 2–H & 20'–H, respectively 2'–H and 4'–H & 20–H indicated an 2*R*,2'*R*,4*S*,4'*R*,20*S*,20'*S* stereochemistry. The sterical proximity of these protons is indicated in crystal structures of tartolons B and C.[17,18] The analogous assignment was confirmed by

nearly identical chemical shifts and signal multiplicities in the NMR data for these parts in **1**. The relative stereochemistry of the C–7/C–8/C–9 and C–7'/C–8'/C–9'/C–11' stereoclusters was addressed by a detailed *J*-based configurational analysis (Figure S3).[19] To determine necessary $^{1}H,^{1}H$ coupling constants in spite of grave overlap of signals in the ^{1}H NMR spectrum, a series of 1D TOCSY NMR experiments irradiating at 23–H_3, 9–H, 11–H, 21–H_3, 23'–H_3, 9'–H and 11'–H was conducted. Strong ROESY correlations between 9–H, 13–OH and methyl 10"–H_3 indicted their axial positions defining a 9*S*,11*R*,13*S* configuration. Finally, the relative configuration between the *trans* epoxide ($J_{H14,H15}$ = 2.8 Hz) and C–13 was established. The large value $^{2}J_{H14C13}$ = 6.6 Hz determined by a *J*-resolved HMBC experiment indicated a *gauge* configuration of 14–H to both oxygens of C–13. In conjunction with the observed ROESY correlations of 14–H to 12–H_b and 15–H to 13–OH and 12–H_a (Figure S2c), this can only be explained by an *eclipsed* configuration of C–12/C–14, and a 13*R*,14*R*,15*R* configuration.

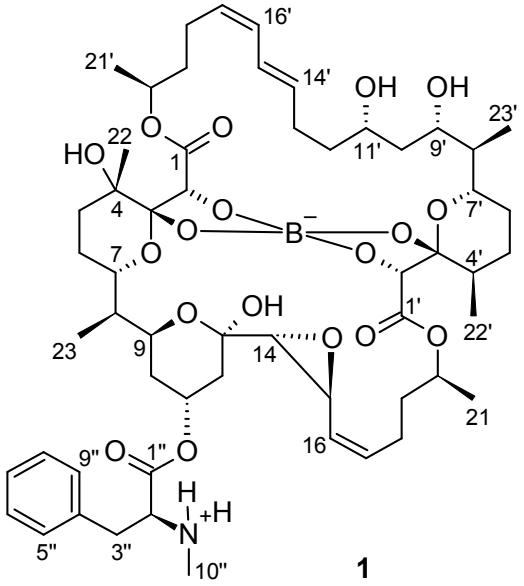

Figure 2. Structure of hyaboron (**1**), a novel asymmetric boron-containing macrodiolide.

Assignment of the absolute stereochemistry of the 9',11'-diol moiety was carried out by Mosher's method. The $\Delta\delta_H$ pattern of the MTPA derivatives (Figure S4) with positive values of 7–H, 8–H, 23–H_3 and negative ones of 12–H_2 to 15––H clearly supports 9'*S*,11'*S* configuration.[20] Because of the dimeric biosynthesis of tartrolon-type metabolites,[21] this also defined the stereochemistry of the second hemisphere and finally showed the same absolute configuration as for tartrolon B, which was established by X-ray data.[22] The absolute configuration of the *N*-methyl-phenylalanine side chain was determined by Marfey's method after alkaline hydrolysis of **1**.[23] Comparison with authentic standards by HPLC-MS analysis finally revealed *S* configuration of C2'' in **1**.

Hyaboron shares its boron binding core structure with a few other boron-containing macrodiolides (see Figure S5). Its closest relative, tartrolon B, was isolated from myxobacterium *Sorangium cellulosum*.[17,22] This small group of structurally related secondary metabolites also includes boromycin *from Streptomyces antibioticus*,[24] aplasmomycin from a marine *S. griseus*,[25] tartrolon C[18] (from *Streptomyces* sp.) and borophycin[26] (from cyanobacterium *Nostoc linckia*). Of these macrodiolides, the only asymmetric representative discovered to date is boromycin.

By HPLC-ESIMS analysis, hyaboron (**1**) could also be detected in crude extracts of *Hyalangium minutum,* strain NOCB-2^{T}, the producer of hyaladione, hyafurones, hyapyrrolines, and hyapyrones.[27,28] This finding might suggest a broad distribution of hyaboron occurrence in the genus *Hyalangium minutum*.

Having elucidated the full structure of hyaboron (**1**), we followed up on the primary screen that was conducted in murine macrophages and investigated the ability of hyaboron and tartrolon B to activate IL-1β in human peripheral blood mononuclear cells (PBMCs). In this set of experiments, we also included boromycin and tartrolon A (without a central boron) alongside the positive control nigericin.[14] Nigericin is a well-characterized antibiotic from *Streptomyces hygroscopicus* that acts as a potassium ionophore. By triggering potassium efflux from cells along the chemical gradient, it acts as a potent activator of the NLRP3 inflammasome.[29] Similar to nigericin, hyaboron, tartrolon B and boromycin induced a considerable IL-1β release into the supernatant of LPS-primed PBMCs (Figure 3A and B). Tartrolon A, however, did not induce IL-1β release. At their maximal effective concentrations, tartrolon B and hyaboron induced approximately 50% of the IL-1β response that was elicited by nigericin, whereas the activity of boromycin was approximately 20% of nigericin. Determining the potency of these compounds by calculating their pEC_{50} (negative logarithm of half maximum effective concentration) revealed that tartrolon B had a pEC_{50} of 6.14±0.15, hyaboron of 7.47±0.09 and boromycin of 7.27±0.12, whereas the positive control nigericin had a pEC_{50} of 8.7±0.02 (Figure 3C).

Similar to nigericin, boromycin has been shown to exert antimicrobial activity through its function as a potassium ionophore.[30] Moreover, tartrolons have also been shown to trigger potassium efflux.[31] As potassium efflux is required upstream of the activation of classical NLRP3 inflammasome activation,[29] we hypothesized that all of the boronated compounds investigated here triggered IL-1β release via activation of the NLRP3 inflammasome. To address this question, we tested the activity of these molecules in the presence of increasing concentrations of extracellular K^+, which has been shown to specifically perturb NLRP3 inflammasome activation by preventing K^+ efflux. In addition, we also included the NLRP3-specific small molecule inhibitor MCC950 in these studies.[32] In order to include dsDNA, as a NLRP3-independent inflammasome stimulus, we conducted these experiments in murine bone marrow derived macrophages (BMDMs).[33] As expected, increasing the extracellular K^+ concentration as well as MCC950 treatment abrogated IL-1β release by nigericin (Figure 3D), whereas activation of the AIM2 (absent in melanoma 2) inflammasome using double stranded DNA was not affected by these treatments. Similarly, increasing extracellular K^+ concentrations or including MCC950 inhibited IL-1β secretion by all boronated macrodiolides. In line with the results obtained in PBMCs, Tartrolon A did not result in maturation of

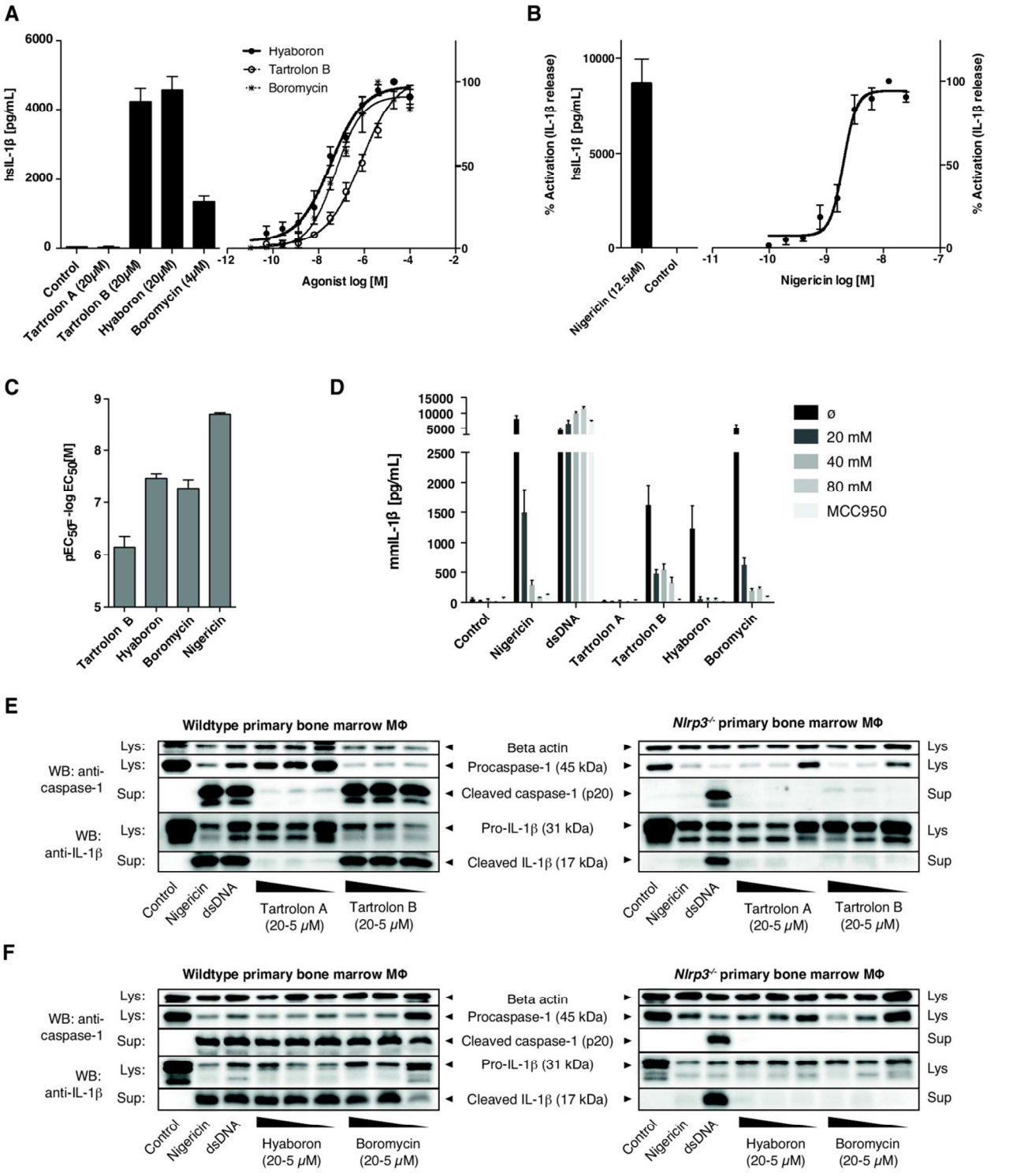

Figure 3. (A-C) Donor PBMCs were primed with LPS for 4 h and stimulated 2 h at the concentrations indicated with the organoborons hyaboron, tartrolon B, and boromycin (A) as well Tartrolon A, which lacks a central boron, and the canonical NLRP3 stimulus nigericin (B). IL-1β was measured in cellular supernatants via ELISA. The graphs display maximal IL-1β release (left) and dose titration as a percentage of the maximum (right) for each compound. For pEC50 determination (C) curve fitting was performed via 4 parameter logistic non-linear regression. Data are mean + SEM (n= 4 donors). (D) Effect of different concentrations of extracellular K+ on IL-1β release. Murine BMDMs were primed with LPS for 4 h and stimulated with nigericin (6.5 μM), dsDNA (1 μg/ml), 20 μM of tartrolon A, B, hyaboron and boromycin in presence of either different concentrations of extracellular K+ or MCC950 (10 μM). After 8 h, IL-1β was measured in cellular supernatants via ELISA. Data are mean + SEM (n= 3) (E, F) Immunoblotting of cleaved IL-1β and cleaved caspase-1 in BMDMs from WT and mice deficient in *Nlrp3*. Cells were primed for LPS for 4 h then stimulated with tartrolon A and B (E) or hyaboron and boromycin (F) as well as the control stimuli dsDNA and nigericin. Cellular lysates (Lys) and supernatants (sup) were then subjected to SDS-PAGE analysis and probed with the indicated antibodies. These data are representative of two independent experiments.

IL-1β in murine BMDMs. Furthermore, investigating caspase-1 and IL-1β maturation by immunoblotting confirmed the results obtained by ELISA. All boronated compounds resulted in the maturation of caspase-1 and IL-1β in wildtype macrophages, similar to the positive controls nigericin and dsDNA (Fig. 3E and F, left panels). Moreover, comparing wildtype and *Nlrp3*-deficient macrophages validated the specific involvement of the NLRP3 inflammasome in the recognition of the boronated compounds. To this end, IL-1β and caspase-1 maturation were completely blunted in *Nlrp3*-deficient macrophages stimulated with nigericin, tartrolon B, hyaboron or boromycin, whereas AIM2-dependent inflammasome activation was fully intact in these cells (Fig. 3E and F, right panels).

Finally, we assessed the activity of hyaboron (**1**) in a number of other biological assays (Table S3). In previous experiments, boron containing compounds were shown to display various biological activities, including antibacterial, antifungal, antiviral, insecticidal, and cytotoxic effects.[34] In addition to its immune-stimulatory activity in mammalian cells, hyaboron (**1**) displayed an antimicrobial effect (minimum inhibitory concentration, MIC, in low µg/mL range) against Gram-positive bacteria and several yeasts and fungi. In addition, we found **1** to inhibit the growth of various human cancer cell lines with half-inhibitory concentrations (IC_{50}) in the nanomolar range. Most interestingly we found that **1** at a concentration as low as 1 µM is a potent inhibitor of parasites that are the causative agents of human African sleeping sickness, Chagas disease, leishmaniasis and malaria, respectively.

Altogether, hyaboron and other boronated compounds likely exhibit their activity via directly or indirectly acting as potassium ionophore.

METHODS

General:

Optical rotation was measured on a Perkin-Elmer 241 spectrometer, the IR spectrum on a Perkin Elmer FT-IR Spectrum 100 spectrometer and the UV spectrum on a Shimadzu UV-Vis spectrophotometer UV-2450. NMR spectra were recorded with Bruker Avance III 700, equipped with 5 mm TCI cryoprobe (^{1}H 700 MHz, ^{13}C 175 MHz), and Bruker DMX 600 (^{1}H 600 MHz, ^{13}C 150 MHz) spectrometers. Chemical shifts δ were referenced to the solvents chloroform-*d* (^{1}H, δ = 7.27 ppm; ^{13}C, δ = 77.0 ppm) and pyridine-d_5 (^{1}H, δ = 7.22 ppm; ^{13}C, δ = 123.9 ppm. ESIMS spectra were acquired on an Amazon ion trap mass spectrometer (Bruker Daltonik); HRESIMS spectra were acquired on a Maxis time-of-flight mass spectrometer (Bruker Daltonik), both combined with an Agilent 1200 series HPLC-UV system [column 2.1 × 50 mm, 1.7 µm, C18 Acquity UPLC BEH (Waters), solvent A: H_2O + 0.1% formic acid; solvent B: ACN + 0.1% formic acid, gradient: 5% B for 0.5 min increasing to 100% B in 19.5 min, maintaining 100% B for 5 min, R_F = 0.6 mL min-1, UV detection 200-600 nm].

Fermentation:

Hyalangium minutum, strain Hym3, was cultivated on a 70 L scale in the presence of 1% Amberlite XAD-16 adsorber resin (Rohm & Haas) in a BR150.3 reactor (100 L operating volume, Chemap AG Switzerland / Bioreactor Baz Nr. 9-4233) at 30 °C in a range of pH 7,1 - 7,3 (adjusted with 10 % KOH / 5,0 % H_2SO_4) at 100 rpm, 0.05 vvm (5,0 NL/min), pO_2: 40 %, V(medium): 5,0 L (5,0 %) for 96 hours in POL/X Medium (Probion 3 g/L, soluble starch 3 g/L, MgSO4 × 7 H_2O 2 g/L, $CaCl_2$ × 2 H_2O 0.5 g/L) behenyl alcohol 150 mg/kg 0.15 g/L, vitamin B_{12} (Cyanocobalamin) 500 µg/L).

Extraction and Isolation:

The XAD resin was eluted with methanol (3 L) and acetone (3 L). Evaporation of the solvents gave an oily extract (17.3 g). The residue was dissolved in ethyl acetate and water and the aqueous layer extracted three times with ethyl acetate. The combined organic layers were evaporated, dried with Na_2SO_4 and evaporated to dryness to yield 7.5 g crude extract. The residue was partitioned between methanol containing 5% water and *n*-heptane. The methanol layer was extracted twice with *n*-heptane to give 2.0 g of a crude methanol extract. Silica gel chromatography (column 120 x 50 mm, Silica gel 60 enriched with 0.1% Ca, Fluka) using 4% methanol in dichloromethane as solvent gave 0.8 g of an enriched product fraction. Subsequent LH-20 chromatography (4.5 x 85 cm) using dichloromethane-methanol 50:50 as eluent at a flow rate of 2.5 mL/min gave 59.6 mg crude product which was further purified in two batches by preparative HPLC on VP250/21 Nucleodur 100-7 C-18 (Machery Nagel); solvent A: 5% acetonitrile in water; solvent B: 95% acetonitrile in water; gradient: 75% B to 100% B in 40 min, then 20 min with 100% B, flow rate 20 mL/min, to give 21.3 mg crude **1**. A second preparative HPLC using isocratic elution with 20% water in acetonitrile for 40 min, then 20 min gradient to 95% acetonitrile, flow rate 20 mL/min, gave 15.6 mg pure product **1**.

Analytical HPLC: r_t = 31.5 min; UV (methanol): λ_{max} (log ε) 227 nm (4.62); $[\alpha]^{20}_D$ +56.2 (c = 1.0, $CHCl_3$); IR (KBr) 3438, 2970, 2932, 1736, 1630, 1457, 1378, 1232, 1196, 1135, 1124, 1100, 1055, 1003, 948, 796, 701 cm^{-1} ; ^{1}H NMR data (700 MHz, $CDCl_3$) δ_H 8.92 (br s, 2''–NH_a), 8.26 (br s, 2''–NH_b), 7.69 (d, *J* = 2.2 Hz, 13–OH), 7.31 (m, 6''–H/8''–H), 7.27 (m, 5''–H/7''–H/9''–H), 6.67 (br s, 11'–OH), 6.18 (m, 16'–H), 6.16 (m, 15'–H), 5.90 (dt, *J* = 14.2, 4.8 Hz, 14'–H), 5.59 (m, 17–H), 5.45 (dd, *J* = 11.4, 2.8 Hz, 16–H), 5.32 (ddd, *J* = 11.0, 9.0, 6.0 Hz, 17'–H), 5.19 (br d, *J* = 12.2 Hz, 2''–H), 5.10 (dt, *J* = 6.0, 3.0 Hz, 11–H), 5.04 (br d, *J* = 12.2 Hz, 9–H), 5.02 (m, 20–H), 4.89 (s, 2–H), 4.83 (br s, 9'–OH), 4.70 (m, 20'–H), 4.68 (s, 2'–H), 3.97 (m, 7–H), 3.93 (m, 7'–H),), 3.79 (br t, *J* = 9.4 Hz, 11'–H), 3.56 (t, *J* = 10.3 Hz, 9'–H), 3.38 (s, 4–OH), 3.28 (dd, *J* = 13.5, 12.2 Hz, 3''–H_a), 3.10 (m, 15–H), 3.05 (br d, *J* = 13.5 Hz, 3''–H_b), 2.94 (m, 18–H_a), 2.88 (br s, 10''–H_3), 2.81 (d, *J* = 2.8 Hz, 14–H), 2.55 (m, 18'–H_a), 2.39 (m, 13'–H_a), 2.16 (m, 13'–H_b), 1.98 (m, 18'–H_b), 1.95 (m, 18–H_b), 1.86 (m, 19'–H_a), 1.84 (br d, *J* = 14.4 Hz, 12–H_a), 1.84 (m, 12'–H_a), 1.82 (m, 4'–H), 1.73 (m, 8'–H), 1.68 (m, 5–H_a, 10–H_a, 19–H_2), 1.67 (ddd, *J* = 14.3, 11.5, 10.0 Hz, 10'–H_a), 1.64 (m, 12'–H_b), 1.57 (m, 12–H_b, 5'–H_2), 1.45 (m, 5–H_b), 1.38 (m, 6–H_2), 1.36 (m, 19'–H_b), 1.35 (s, 22–H_3), 1.23 (br d, *J* = 14.3 Hz, 10'–H_b), 1.23 (br d, *J* = 13.3 Hz, 10–H_b), 1.22 (d, *J* = 6.2 Hz, 21–H_3), 1.16 (m, 8–H), 1.09 (m, 6'–H_2), 1.07 (d, *J* = 6.2 Hz, 21'–H_3), 0.99 (d, *J* = 6.7 Hz, 22'–H_3), 0.77 (d, *J* = 7.5 Hz, 23'–H_3),0.76 (d, *J* = 7.5 Hz, 23–H_3); ^{13}C NMR data (175 MHz, $CDCl_3$) δ_C 173.5 (C, C–1'), 173.4 (C, C–1), 165.6 (C, C–1''), 135.6 (CH, C–14'), 135.1 (CH, C–4''), 134.5 (CH, C–17), 131.2 (CH, C–16'), 129.8 (CH, C–5''/ C–9''), 128.7 (CH, C–6''/ C–8''), 128.1 (CH, C–17'), 127.3 (CH, C–7''), 124.3 (CH, C–16), 123.2 (CH, C–15'), 104.8 (C, C–3), 103.5 (C, C–3'), 93.9 (C, C–13), 80.3 (CH, C–9'), 78.0 (CH, C–2), 77.2 (CH, C–2'),

76.0 (CH, C–11'), 72.1 (C, C–4), 71.8 (CH, C–7'), 71.5 (CH, C–11), 69.1 (CH, C–20'), 68.4 (CH, C–20), 68.3 (CH, C–7), 61.59 (CH, C–9), 61.56 (CH, C–14), 59.9 (CH, C–2''), 52.1 (CH, C–15), 43.2 (CH, C–8'), 41.6 (CH, C–8), 35.5 (CH_2, C–19'), 34.63 (CH_2, C–5), 34.60 (CH_2, C–10'), 34.59 (CH_2, C–19), 34.4 (CH, C–4'), 33.9 (CH_2, C–12'), 33.2 (CH_2, C–12), 32.2 (CH_3, C–10''), 32.0 (CH_2, C–10), 31.3 (CH_2, C–3''), 30.5 (CH_2, C–6'), 29.0 (CH_2, C–5'), 28.7 (CH_2, C–13'), 25.2 (CH_2, C–6), 25.0 (CH_3, C–22), 23.1 (CH_2, C–18'), 22.6 (CH_2, C–18), 20.7 (CH_3, C–21), 20.3 (CH_3, C–21'), 16.9 (CH_3, C–22'), 14.5 (CH_3, C–23'), 8.1 (CH_3, C–23); HRESIMS: *m/z* 1068.5710 $[M + H]^+$ (calcd for $C_{56}H_{83}BNO_{18}$ $[M + H]^+$ 1068.5707).

Preparation of the (*S*)- and (*R*)-MTPA ester derivatives of hyaboron (1)

For the (*S*)-MTPA ester derivative hyaboron (**1**) (3.9 mg, 3.7 µmol) was dissolved in dry dichloromethane (350 µL) and DMAP (3.9 mg), triethylamine (22 µL) and *R*-(-)-MTPA-chloride (22 µL) were added at 0 °C and stirred under argon atmosphere at room temperature for 24 h. The reaction mixture was quenched at 0 °C with buffer solution (pH 7) and extracted three times with dichloromethane, dried over $MgSO_4$ and concentrated in *vacuo* to dryness. The crude product was purified by silica gel chromatography (1 x 12.5 cm) using *tert*.-butyl-methyl ether/*n*-heptane 2:3, then 1:1 as solvent. The *S*-MTPA derivative **1a** was further purified by preparative RP-HPLC chromatography on Nucleosil 100-7 (250 x 4) (Machery Nagel) using *n*-heptane/*tert*.-butyl-methyl ether 85:15 containing 1% methanol as solvent, flow rate 20 mL/min to yield 1.7 mg of compound **1a** (*m/z* 1715.68). ^{1}H NMR data (600 MHz, $CDCl_3$) of **1a**: similar to **1**, but δ_H 6.28 (15'–H), 5.59 (14'–H), 5.19 (11'–H), 5.02 (9'–H), 3.91 (7'–H), 2.05 (13'–H_a), 1.92 (10'–H_2), 1.75 (13'–H_b), 1.75 (12'–H_2), 1.69 (8'–H), 0.75 (23'–H_3).

The (*R*)-MTPA-ester of **1** was prepared analogously from 4.8 mg (4.5 µmol) of **1** to give 2.4 mg of compound **1b**. ^{1}H NMR data (600 MHz, $CDCl_3$) of **1b**: similar to **1**, but δ_H 6.32 (15'–H), 5.70 (14'–H), 5.22 (11'–H), 5.09 (9'–H), 3.72 (7'–H), 2.21 (13'–H_a), 2.09 (10'–H_a), 1.96 (12'–H_2), 1.95 (13'–H_b), 1.85 (10'–H_b), 1.66 (8'–H), 0.66 (23'–H_3).

Preparation and Analysis of L-FDAA-Derivatives

Hyaboron (**1**, 0.5 mg, 0.5 µmol) was dissolved in methanol (150 µL) and hydrolyzed with 1 N sodium hydroxide (5 µL) for 10 min. 1 N aqueous HCl (5 µL) was added and the reaction mixture diluted with 50 µL H_2O. After addition of 1 N $NaHCO_3$ (5 µL) and 1% L-FDAA in acetone (20 µL) the reaction mixture was heated at 40 °C for 1 h. The reaction was quenched with 1 N HCl (5 µL) and evaporated to dryness. The residue was dissolved in H_2O (100 µL) and analyzed by RP-HPLC-MS using a gradient of 5% B to 50% B in 20 min (eluent A: H_2O/CH_3CN 95:5, 0.1% formic acid, eluent B: CH_3CN/H_2O 95:5, 0.1% formic acid; flow: 0.6 mL/min); *m/z* 431.14; retention time (min) of FDAA-derivatized amino acid standards (Bachem): *N*-Me-PheOH 14.0 min; *N*-Me-D-PheOH 14.1 min.

Assays for Antimicrobial and Cytotoxic Activities

Minimum inhibitory concentrations (MIC) were determined (Table S1) in 96-well microtiter plates in a serial dilution assay with EBS medium as previously described.[35]

Cytotoxicity assay

In vitro cytotoxicity (IC_{50}) was determined against different cell lines using our protocol described previously.[35]

PBMCs isolation

PBMCs were isolated from human buffy coats using standard protocol.[33] In short, cells were separated by density gradient centrifugation using Biocoll separating solution (Biochrom) followed by short erythrocyte lysis using BD pharm Lyse.

BMDMs preparation

Bone marrow was isolated from femur and tibia of either wild type or *Nlrp3* deficient C57BL/6 mice.[14] Cells were filtered and subjected to erythrocyte lysis. As described previously, bone marrow was differentiated in macrophages using 30% L929 supernatant in DMEM for seven days.[36]

Primary Screening (iGLuc)

Primary screening was performed with J774 macrophages stably expressing iGluc reporter system with constitutive expression of NLRP3 under EF1α promotor.[37] On the day of the experiment, 30,000 cells were plated in each well in a 384-well plate with the help of multidrop reagent dispenser (Thermo Fisher Scientific). After 2 h, cells were stimulated with natural compound library (NCL; DZIF) at 1 µM concentration. Compounds were transferred onto the cells using high density replication tool (with pre-determined transfer capacity) in Biomek FXP laboratory automation workstation (Beckman Coulter). 2 h after stimulation, the gaussia signal was measured in the supernatant by adding coelenterazine at a final concentration of 1µg/mL and measuring luminescence using the Envision multilabel reader (Perkin Elmer).

Stimulations

Human PBMCs were primed with 25 pg/ml of ultrapure LPS from E. coli (Invivogen) for 4 h. Stimulation was performed with indicated concentrations of stimuli for 2 h. Mouse BMDMs were primed with 200 ng/ml of LPS for 4 h followed by stimulation with indicated stimuli for 8 h. For double stranded DNA (dsDNA), pBlueScript plasmid DNA (1 µg/ml) was complexed with Lipofectamine 2000 (Life Technologies) according to the manufacturer's protocol. In the high extracellular potassium experiment, medium was diluted with 150 mM potassium chloride to the indicated potassium concentrations. When indicated, the NLRP3 inhibitor MCC950 (10 µM) was added in last hour of priming.

Immunoblotting and ELISA assay

For immunoblotting, $1x10^6$ cells were plated per well in a 12-well plate and stimulations were performed as described above. Supernatants were precipitated using methanol-

chloroform extraction and immunoblotting was performed as described previously.[38] Primary antibodies for IL-1β (AF-401-NA) and caspase 1 (AG-20B-0042-C100) were purchased from R&D systems and Adipogen, respectively. Beta-actin and secondary antibodies were purchased from Santa Cruz. For human and mouse IL-1β ELISA (BD Bioscience), $1x10^5$ cell per well were plated in a 96-well flat bottom plate. After stimulation, the cytokine IL-1β was measured in the cellular supernatant according to manufacturer's instructions.

ASSOCIATED CONTENT

Supporting Information. Complete experimental details and spectral data is available free of charge via the Internet at http://pubs.acs.org.

AUTHOR INFORMATION

Corresponding Authors

* Email: hornung@genzentrum.lmu.de.
* Email: rom@helmholtz-hzi.de.

ORCID

Frank Surup: 0000-0001-5234-8525

Eva Bartok: 0000-0003-0556-1950

Marc Stadler: 0000-0002-7284-8671

Rolf Müller: 0000-0002-1042-5665

Present addresses

▽Bayer AG, Pharmaceuticals Research & Development, Friedrich-Ebert-Str. 217-333, 42096 Wuppertal, Germany.

○Cargill GmbH, Seehafenstr. 2, 21079 Hamburg, Germany.

Author Contributions

+These authors made equal contributions.
The manuscript was written through contributions of all authors. / All authors have given approval to the final version of the manuscript.

Funding Sources

EB received financial support from BONFOR (University of Bonn). DC and VH were supported by DZIF funds.

Notes

The authors declare no competing financial interest.

ACKNOWLEDGMENT

We kindly thank V. Dixit for *Nlrp3*-deficient mice (Genentech, USA), C. Kakoschke for recording NMR spectra, A. Gollasch und H. Steinmetz for MPLC-HRESIMS measurements, K. P. Conrad for technical assistance, W. Collisi for conducting bioas-says, K. Mohr for the toc picture, W. Kessler and co-workers for large scale fermentations, M. Kaiser (Swiss TPH) for antiparasitic assays, and Rolf Jansen for proofreading of the manuscript.

ABBREVIATIONS

PRR, pathogen recognition receptors; PAMP, pathogen associated molecular patterns; DAMP, danger associated molecular pattern; NLR, NOD-like receptor; ASC, apoptosis associated speck like protein containing caspase activation and recruitment domain; IL-1β, interleukin-1β; PBMC, blood mononuclear cell.

REFERENCES

(1) Medzhitov, R. (2007) Recognition of microorganisms and activation of the immune response. *Nature 449*, 819–826.
(2) Kohanski, M. A., Dwyer, D. J., Collins, J. J. (2010) How antibiotics kill bacteria: from targets to networks. *Nat. Rev. 8*, 423–435.
(3) Coates A. R. M., Halls, G., Hu, Y. (2011) Novel classes of antibiotics or more of the same? *Br. J. Pharmacol. 163*, 184–194.
(4) Maxson, T., Mitchell, D. A. (2016) Targeted treatment for bacterial infections: prospects for pathogen-specific antibiotics coupled with rapid diagnostics. *Tetrahedron 72*, 3609–3624.
(5) Helbig, E. T., Opitz, B., Sander, L. E. (2013) Adjuvant immunotherapies as a novel approach to bacterial infections. *Immunotherapy 5*, 365–381.
(6) Bauernfeind, F. G., Hornung, V. (2013) Of inflammasomes and pathogens – sensing of microbes by the inflammasome. *EMBO Mol. Med. 5*, 814–816.
(7) Broz, P., Dixit, V.M. (2016) Inflammasomes: mechanism of assembly, regulation and signalling. *Nat. Rev. Immunol. 16*, 407–420.
(8) Bauernfeind, F. G., Horvath, G., Stutz, A., Alnemri, E. S., MacDonald, K., Speert, D., Fernandes-Alnemri, T., Wu, J., Monks, B. G., Fitzgerald, K. A., Hornung, V., Latz, E. (2009) Cutting edge: NF-κB activating pattern recognition and cytokine receptors license NLRP3 inflammasome activation by regulating NLRP3 expression. *J. Immunol. 183*, 787–791.
(9) Juliana, C., Fernandes-Alnemri, T., Kang, S., Farias, A., Qin, F., Alnemri, E. S. (2012) Non-transcriptional priming and deubiquitination regulate NLRP3 inflammasome activation. *J. Biol. Chem. 287*, 36617–36622.
(10) Bartok, E., Bauernfeind, F. G., Khaminets, M. G., Jakobs C., Monks, B. G., Fitzgerald, K. A., Latz, E., Hornung, V. (2009) iGLuc: a luciferase-based inflammasome and protease activity reporter. *Nat Methods 10*, 147–154.
(11) Bartok, E., Kampes, M., Hornung, V. (2016) Measuring IL-1β Processing by Bioluminescence Sensors II: The iGLuc System. *Methods Mol. Biol. 1417*, 97–113.
(12) Bauernfeind, F., Bartok, E., Rieger, A., Franchi, L., Núñez, G., Hornung, V. (2011) Cutting edge: reactive oxygen species inhibitors block priming, but not activation, of the NLRP3 inflammasome. *J. Immunol. 187*, 613–617.
(13) Cheneval, D., Ramage, P., Kastelic, T., Szelestenyi, T., Niggli, H., Hemmig, R., Bachmann, M., MacKenzie, A. (1998) Increased mature interleukin-1β (IL-1β) secretion from THP-1 cells induced by nigericin is a result of activation of p45 IL-1β-converting enzyme processing. *J. Biol Chem. 273*, 17846–17851.
(14) Mariathasan, S., Weiss, D. S., Newton, K., McBride, J., O'Rourke, K., Roose-Girma, M., Lee, W. P., Weinrauch, Y., Monack, D. M., Dixit, V. M.. (2006) Cryopyrin activates the inflammasome in response to toxins and ATP. *Nature. 440*, 228–232.
(15) Zhang, J.-H., Chung, T. D. Y., Oldenburg, K. R. (1999) A Simple Statistical Parameter for Use in Evaluation and Validation of High Throughput Screening Assays, *J. Biomol. Screen. 4*, 67–73.
(16) Schummer, D.; Forche, E.; Wray, V.; Domke, T.; Reichenbach, H.; Höfle, G (1996) Antibiotics from gliding bacteria, LXXVI. Vioprolides: New antifungal and cytotoxic peptolides from *Cystobacter violaceus*. *Liebigs Ann. 1996*, 971–978.
(17) Schummer, D.; Irschik, H.; Reichenbach, H.; Höfle, G (1994) Antibiotics from gliding bacteria, LVII. Tartrolons: New boron-containing macrodiolides from *Sorangium cellulosum*. *Liebigs Ann. 1994*, 283–289.

(18) Lewer, P.; Chapin, E. L.; Graupner, P. R.; Gilbert, J. R.; Peacock, C. J. (2003) Tartrolone C: A novel insecticidal macrodiolide produced by *Streptomyces* sp. CP1130. *Nat. Prod. 66*, 143–145.

(19) Matsumori, N.; Kaneno, D.; Murata, M.; Nakamura, H.; Tachibana, K. (1999) Stereochemical determination of acyclic structures based on carbon-proton spin-coupling constants. A method of configuration analysis for natural products. *J. Org. Chem. 64*, 866–876.

(20) Seco, J. M.; Quiñoá, E.; Riguera, R. (2012) Assignment of the absolute configuration of polyfunctional compounds by NMR using chiral derivatizing agents. *Chem. Rev.* **2012**, *112*, 4603–4641.

(21) Elshahawi, S. I.; Trindade-Silva, A. E.; Hanora, A.; Han, A. W.; Flores, M. S.; Vizzoni, V.; Schrago, C. G.; Soares, C. A.; Concepcion, G. P.; Distel, D. L.; Schmidt, E. W.; Haygood, M. G. (2013) Boronated tartrolon antibiotic produced by symbiotic cellulose-degrading bacteria in shipworm gills. *Proc. Natl. Acad. Sci. 110*, E294–E304.

(22) Schummer, D.; Schomburg, D.; Irschik, H.; Reichenbach, H.; Höfle, G. (1996) Antibiotics from gliding bacteria, LXXV. Absolute configuration and biosynthesis of tartrolon B, a boron-containing macrodiolide from *Sorangium cellulosum. Liebigs Ann. 1996*, 965–969.

(23) Harada, K.; Fuji, K.; Hayashi, K.; Suzuki M. (1996) Application of D,L-FDLA derivatization to determination of absolute configuration of constituent amino acids in peptide by advanced Marfey's method, *Tetrahedron Lett. 37*, 3001–3004.

(24) Dunitz, J. D.; Hawley, D. M.; Miklos, D.; White, D. N. J.; Berlin, Y.; Marusic, R.; Prelog, V. (1971) Structure of boromycin. *Helv. Chim. Acta 54*, 1709–1713; Somers, T. C.; White, J. D.; Lee, J. J.; Keller, P. J.; Chang, C.; Floss, H. G. (1986) A NMR analysis of boromycin sodium complex and sodium desvalinoboromycinate. *J. Org. Chem.*, *51*, 464–471; Pache, W.; Zahner, H. (1969) Metabolic products of microorganisms 77. Studies on the mechanism of action of boromycin. *Arch. Mikrobiol.*, *67*, 156–165.

(25) Okami, Y.; Okazaki, T.; Kitahara; T.; Umezawa H. (1976*)* Studies on marine microorganisms V. A new antibiotic, aplasmomycin, produced by a Streptomycete isolated from shallow sea mud. *J. Antibiot.*, *24*, 1019–1025.

(26) Hemscheidt, T.; Puglisi, Larsen, L. K.; Patterson, G. M. L.; Moore, R. E. (1994) Structure and biosynthesis of borophycin a new boeseken complex of boric acid from a marine strain of the blue-green alga *Nostoc linckia*. *J. Org. Chem.*, *59*, 3467–3471.

(27) Okanya, P. W.; Mohr, K. I.; Gerth, K.; Steinmetz, H.; Huch, V.; Jansen, R.; Müller, R. (2012) Hyaladione, an S-methyl cyclohexadiene-dione from *Hyalangium minutum. J. Nat. Prod. 75*, 768–770.

(28) Okanya, P. W.; Mohr, K. I.; Gerth, K.; Kessler, W.; Jansen, R.; Stadler, M.; Müller, R. (2014) Hyafurones, hyapyrrolines, and hyapyrones: polyketides from *Hyalangium minutum*. *J. Nat. Prod. 77*, 1420–1429.

(29) Muñoz-Planillo, R., Kuffa, P., Martínez-Colón, G., Smith, B. L., Rajendiran, T.M., Núñez, G. (2013) K^+ efflux is the common trigger of NLRP3 inflammasome activation by bacterial toxins and particulate matter. Immunity 38, 1142–1153.

(30) Moreira, W.; Aziz, D. B.; Dick, T. (2016) Boromycin kills mycobacterial persisters without detectable resistance. *Front. Microbiol*. *7*, 199.

(31) Irschik, H., Schummer, D., Gerth, K., Höfle, G., Reichenbach, H. (1995) The tartrolons, new boron-containing antibiotics from a myxobacterium, *Sorangium cellulosum*. *J. Antibiot. 48*, 26–30.

(32) Coll, R. C., Robertson, A. A., Chae, J. J., Higgins, S. C., Muñoz-Planillo, R., Inserra, M. C., Vetter, I., Dungan, L. S., Monks, B. G., Stutz, A., Croker, D. E., Butler, M. S., Haneklaus, M., Sutton, C. E., Núñez, G., Latz, E., Kastner, D. L., Mills, K. H., Masters, S. L., Schroder, K., Cooper, M. A., O'Neill, L. A. (2015) A small-molecule inhibitor of the NLRP3 inflammasome for the treatment of inflammatory diseases. *Nat. Med. 21*, 248–255.

(33) Gaidt, M. M., Ebert, T. S., Chauhan, D., Ramshorn, K., Pinci, F., Zuber, S., O'Duill, F., Schmid-Burgk, J. L., Hoss, F., Buhmann, R., Wittmann, G., Latz, E., Subklewe, M., Hornung, V. (2017) The DNA inflammasome in human myeloid cells is initiated by a STING-cell death program upstream of NLRP3. *Cell 171*, 1110–1124.

(34) Řezanka, T.; Sigler, K. (2008) Biologically active compounds of semi-metals. *Phytochemistry 69*, 585–606.

(35) Surup, F.; Thongbai, B.; Kuhnert, E.; Sudarman, E.; Hyde, K. D.; Stadler, M. (2015) Deconins A-E: Cuparenic and mevalonic or propionic acid conjugates from the basidiomycete deconica sp. 471. *J. Nat. Prod. 78*, 934-938.

(36) Gaidt, M. M., Ebert, T. S., Chauhan, D., Schmidt, T., Schmid-Burgk, J. L., Rapino, F., Robertson, A. A., Cooper, M. A., Graf, T., Hornung V. (2016) Human monocytes engage an alternative inflammasome pathway. *Immunity 19*, 833–846.

(37) Bartok, E., Bauernfeind, F., Khaminets, M. G., Jakobs, C., Monks, B., Fitzgerald, K. A., Latz, E., Hornung V (2013) iGLuc: a luciferase-based inflammasome and protease activity reporter. *Nat. Methods 10*, 147–154.

(38) Jakobs, C., Bartok, E., Kubarenko, A., Bauernfeind, F., Hornung V (2013) Immunoblotting for active caspase-1. *Methods Mol Biol.1040*, 103–115.

Insert Table of Contents artwork here